The EMBO Journal (2005) 24, 4271–4278 | © 2005 European Molecular Biology Organization | All Rights Reserved 0261-4189/05
www.embojournal.org

THE EMBO JOURNAL

Regulation of G_0 entry by the Pho80–Pho85 cyclin–CDK complex

Valeria Wanke[1], Ivo Pedruzzi[1], Elisabetta Cameroni[1], Frédérique Dubouloz and Claudio De Virgilio*

Department of Microbiology and Molecular Medicine, CMU, University of Geneva, Geneva, Switzerland

Eukaryotic cell proliferation is controlled by growth factors and essential nutrients. In their absence, cells may enter into a quiescent state (G_0). In *Saccharomyces cerevisiae*, the conserved protein kinase A (PKA) and rapamycin-sensitive TOR (TORC1) pathways antagonize G_0 entry in response to carbon and/or nitrogen availability primarily by inhibiting the PAS kinase Rim15 function. Here, we show that the phosphate-sensing Pho80–Pho85 cyclin–cyclin-dependent kinase (CDK) complex also participates in Rim15 inhibition through direct phosphorylation, thereby effectively sequestering Rim15 in the cytoplasm via its association with 14-3-3 proteins. Inactivation of either Pho80–Pho85 or TORC1 causes dephosphorylation of the 14-3-3-binding site in Rim15, thus enabling nuclear import of Rim15 and induction of the Rim15-controlled G_0 program. Importantly, we also show that Pho80–Pho85 and TORC1 converge on a single amino acid in Rim15. Thus, Rim15 plays a key role in G_0 entry through its ability to integrate signaling from the PKA, TORC1, and Pho80–Pho85 pathways.

The EMBO Journal (2005) **24,** 4271–4278. doi:10.1038/sj.emboj.7600889; Published online 24 November 2005
Subject Categories: signal transduction; cellular metabolism
Keywords: G_0; nutrient starvation; Pho80–Pho85 cyclin–CDK complex; Rim15; TORC1

Introduction

Eukaryotic signal transduction pathways convert extracellular cues such as growth factors, hormones, and/or nutrients to intracellular signals which, following proper integration, determine the decision between cell proliferation and entry into a nondividing resting state, termed quiescence (G_0). In the yeast *Saccharomyces cerevisiae*, the PKA and TORC1 signaling pathways, which positively regulate cell proliferation in response to nutrient availability, are key determinants of G_0 entry (Thevelein and de Winde, 1999; Gray *et al*, 2004; Martin and Hall, 2005). As a consequence, inactivation of either of these major pathways results in a G_0-like growth arrest phenotype, even in the presence of abundant nutrients. Recent evidence suggests that the signal flow through both pathways is integrated at various levels. For instance, TORC1 depletion was proposed to favor the formation of an inactive nuclear PKA/Bcy1 holoenzyme (Schmelzle *et al*, 2004). In addition, both PKA and TORC1 converge on common target proteins, such as the stress response transcription factors Msn2/4, as well as Rim15 (Schneper *et al*, 2004). Rim15 is a distinct member of the PAS kinase family, which functions as a key controller of many aspects of the G_0 program (including G_1 cell cycle arrest, glycogen and trehalose synthesis, and activation of Gis1- and/or Msn2/4-dependent transcription (e.g. of *HSP26* and *GRE1*; Reinders *et al*, 1998; Pedruzzi *et al*, 2000, 2003; Cameroni *et al*, 2004).

Entry into a G_0-like state can also be triggered by phosphate starvation (Lillie and Pringle, 1980), albeit the corresponding regulatory mechanisms are largely unknown (Gray *et al*, 2004). The primary nutrient-signaling kinase that orchestrates the phosphate starvation response is Pho85, a CDK that associates with a family of 10 cyclins, each of which can potentially direct Pho85 to different target substrates (Carroll and O'Shea, 2002). The best-studied partner of Pho85 is the cyclin Pho80. It has previously been shown that the Pho80–Pho85 cyclin–CDK complex regulates the phosphate starvation response by controlling both the localization and activity of the transcription factor Pho4. Pho4, in turn, activates transcription of phosphate acquisition genes (Carroll and O'Shea, 2002). Interestingly, several studies indicate that Pho85 negatively controls the expression of an additional set of genes (including glycogen and trehalose synthesis, oxidoreductive stress, and protein folding genes) that are typically induced under glucose-limiting conditions prior to entry into G_0 (DeRisi *et al*, 1997; Timblin and Bergman, 1997; Ogawa *et al*, 2000; Carroll *et al*, 2001; Nishizawa *et al*, 2004). These findings suggest that proper execution of the G_0 program also includes integration of the Pho85-mediated phosphate signal.

The work presented here pinpoints Rim15 as a key target of the Pho85 signaling pathway. Results from physiologic, genetic and biochemical studies indicate that Rim15 is a Pho80–Pho85 kinase substrate and that the resulting phosphorylation of Rim15 favors its cytoplasmic retention via association with the 14-3-3 protein Bmh2. Our data further demonstrate that this regulation is important for proper control of G_0 entry in response to phosphate availability. Interestingly, inactivation of either Pho80–Pho85 or TORC1 leads to dephosphorylation of the 14-3-3 binding site in Rim15, suggesting that both signaling pathways converge on a single amino acid in Rim15 to regulate its nucleocytoplasmic distribution.

Results and discussion

Protein kinase activity of Rim15 is critical for its nuclear export

As part of our continued efforts to define in detail the molecular mechanism of Rim15 function, we asked whether

*Corresponding author. Department of Microbiology & Molecular Medicine, CMU, University of Geneva, 1211 Geneva, Switzerland.
Tel.: +41 22 379 54 95; Fax: +41 22 379 55 02;
E-mail: Claudio.DeVirgilio@medecine.unige.ch
[1]These authors contributed equally to this work

Received: 12 August 2005; accepted: 4 November 2005; published online: 24 November 2005

the Rim15 kinase activity itself plays a role in its subcellular localization. To address this question, we analyzed the localization of kinase-inactive GFP-Rim15^{K823Y} and GFP-Rim15^{C1176Y} fusion proteins (see Materials and methods for further details) in *rim15*Δ cells. We found that GFP-Rim15^{K823Y} and GFP-Rim15^{C1176Y}, but not GFP-Rim15, accumulated in the nuclei of rapamycin-treated or glucose-limited *rim15*Δ cells (Figure 1A). Furthermore, when such rapamycin-treated or glucose-limited *rim15*Δ mutant cells were respectively re-supplied with nutrient-rich medium or released from the rapamycin block (both in the presence of the translation inhibitor cycloheximide), GFP-Rim15^{K823Y} and GFP-Rim15^{C1176Y}, but not GFP-Rim15, remained predominantly in the nucleus (data not shown). The simplest interpretation of these results is that the kinase activity of Rim15 is required for its efficient export from the nucleus. Moreover, from a collection of importin β-related, nuclear-transport-receptor mutants tested, only the *msn5*Δ mutant showed both GFP-Rim15^{C1176Y} and GFP-Rim15^{K823Y} constitutively localized in the nucleus (Figure 1B). Thus, our data indicate that the kinase activity of Rim15 is needed for its efficient, Msn5-driven nuclear export and show that GFP-tagged kinase-inactive Rim15 variants are useful tools in the study of nutrient-regulated cytoplasmic retention and/or nuclear import of Rim15.

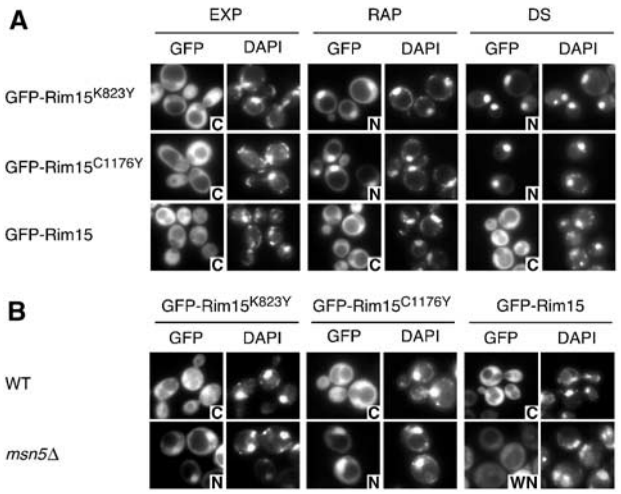

Figure 1 Protein kinase-inactivating mutations permit the study of cytoplasmic retention and/or nuclear import of GFP-Rim15. (**A**) Localization of GFP-Rim15^{K823Y}, GFP-Rim15^{C1176Y}, and GFP-Rim15. Exponentially growing (EXP), rapamycin-treated (RAP), and diauxic (DS; $OD_{600} = 3.5$) *rim15*Δ (IP31) cells expressing GFP-Rim15^{K823Y} (pFD1008), GFP-Rim15^{C1176Y} (pFD633), or GFP-Rim15 (pFD846) were visualized by fluorescence microscopy. (**B**) Localization of GFP-Rim15^{K823Y} (pFD1008), GFP-Rim15^{C1176Y} (pFD633), or GFP-Rim15 (pFD846) in exponentially growing wild-type (W303-1A) or *msn5*Δ (YBL029) cells. Notably, the *msn5*Δ mutant overexpressing GFP-Rim15 was very sick, which is consistent with the expectation that overproduction (from the *ADH1* promoter) of nuclear GFP-Rim15 wild-type protein is detrimental to cell growth. Nevertheless, the overall very weak GFP-Rim15 signal observed in these cells was for the most part localized in the nuclei (WN, weak nuclear staining). N and C denote mainly nuclear and cytoplasmic localization of the GFP-fusion proteins, respectively.

Cytoplasmic retention of GFP-Rim15 depends on its association with 14-3-3 proteins

Rim15 is a distant member of the NDR family of AGC kinases, which share the unique feature of harboring an insert of at least 30 amino acids between the protein kinase subdomains VII and VIII (Tamaskovic *et al*, 2003; Cameroni *et al*, 2004). Although the function of this insert segment is not well understood, at least in the case of NDR1, it is known to contain a nonconsensus nuclear localization signal (Tamaskovic *et al*, 2003). Interestingly, the corresponding kinase insert in Rim15 contains neither a consensus nor a nonconsensus NDR1 nuclear localization signal, but instead harbors (flanking amino-acid residue Thr^{1075} [T1075]) the single high-stringency 14-3-3-binding motif in Rim15 (RSXpS/TXP; Figure 2A; Yaffe *et al*, 2001).

Several observations point to a role for the yeast 14-3-3 proteins Bmh1/2 in the nutrient-controlled nuclear exclusion of Rim15, possibly by a similar mechanism as previously described for the transcription factors Msn2/4 and the DYRK-family kinase Yak1 (Beck and Hall, 1999; Moriya *et al*, 2001). First, when fused to GST, the kinase insert of Rim15 (Rim15^{KI}) bound Bmh2-HA^3 in co-immunoprecipitation (co-IP) experiments (Figure 2B). Importantly, this interaction was largely disrupted by introducing a T1075A mutation in Rim15^{KI}, which abolishes the presumed phosphothreonine (pT) residue critical for regulation of 14-3-3-protein–protein interactions (Yaffe *et al*, 2001). Second, while GFP-Rim15^{C1176Y} was rarely found in the nuclei of exponentially growing cells (i.e. in $<1\%$ of the cells), introduction of the T1075A mutation or deletion of the entire kinase insert in GFP-Rim15^{C1176Y} caused the corresponding fusion proteins to constitutively localize in the nuclei of 40 or 68% of the cells, respectively (Figure 2C). The slightly more robust constitutive nuclear localization of GFP-Rim15$^{C1176Y/\Delta KI}$ suggests that additional domains in the kinase insert of Rim15 may participate in the cytoplasmic retention of Rim15 (see below). Third, the switch from galactose to glucose-rich medium of a strain in which the only source of Bmh protein was provided by *BMH2* under the control of the *GAL1* promoter resulted in the expected depletion of Bmh2 (Figure 2D), and was paralleled by the nuclear accumulation of GFP-Rim15^{C1176Y} (Figure 2E). In a strain carrying a genomic wild-type copy of *RIM15*, this nuclear localization resulted in the Rim15-dependent transcriptional activation of *GRE1* and *HSP26* (Figure 2F; notably, Bmh protein depletion caused a weak, transient activation of *HSP26* even in the absence of Rim15, indicating that Bmh proteins regulate *HSP26* transcription in part also via a Rim15-independent process). Interestingly, in this context, we found that 27 of the 76 genes that were reported to be induced following Bmh1/2 depletion (Ichimura *et al*, 2004), were also included in the set of genes that required Rim15 for induction at the diauxic shift (Cameroni *et al*, 2004). Taken together, our findings indicate that the association between Bmh1/2 proteins and the pT1075 14-3-3-binding site in Rim15 can account for the cytoplasmic retention of GFP-Rim15 in exponentially growing cells.

The Pho80–Pho85 cyclin–CDK complex phosphorylates T1075 in Rim15

The T1075 amino acid of Rim15 is not only a critical residue of the 14-3-3 binding site, but is also part of a proposed Pho85 consensus phophorylation sequence S/TPXI/L (Figure 2A; O'Neill *et al*, 1996). This suggested to us that Pho85 may phosphorylate T1075 in Rim15. In support of this assump-

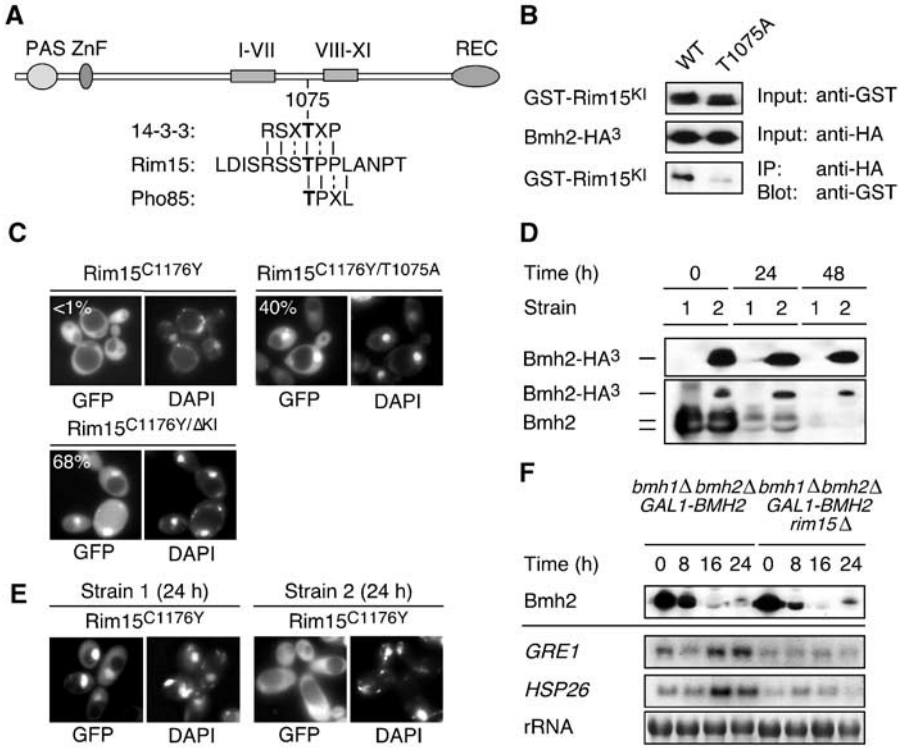

Figure 2 Cytoplasmic retention of GFP-Rim15 depends on its association with 14-3-3 proteins. (**A**) Domain architecture of Rim15. The various domains of Rim15 include the N-terminal PAS, the C_2HC-type zinc-finger (ZnF), the central kinase catalytic domain (gray rectangles) with an insert of 188 amino acids between subdomains VII and VIII, and the C-terminal receiver (REC) domain. As predicted by the Scansite program (http://scansite.mit.edu) the single high-stringency, putative 14-3-3 protein-binding site in Rim15 (scoring in the top 0.165%) flanks amino-acid T1075. (**B**) Interaction between $Rim15^{KI}$ and Bmh2. $Bmh2\text{-}HA^3$ (pTB419) was immunoprecipitated from extracts prepared from wild-type cells (W303-1A) expressing either GST-$Rim15^{KI}$ (pVW900) or GST-$Rim15^{KI\text{-}T1075A}$ (pVW902). The input extracts (upper two panels) and the immunoprecipitates (lower panel) were analyzed via immunoblot analysis using anti-GST (upper and lower panels) or anti-HA antibodies (panel in the middle). (**C**) Localization of GFP-$Rim15^{C1176Y}$ (pFD633), GFP-$Rim15^{C1176Y/T1075A}$ (pVW1017), and GFP-$Rim15^{C1176Y/\Delta KI}$ (pVW1068) in exponentially growing *rim15*Δ (IP31) cells. The numbers indicate the percentage of cells with clear nuclear staining of the GFP-fusion protein; >200 cells were counted. (**D, E**) Depletion of 14-3-3 proteins results in the nuclear accumulation of GFP-$Rim15^{C1176Y}$. GFP-$Rim15^{C1176Y}$ (pFD633) expressing *bmh1*Δ *bmh2*Δ *rim15*Δ [*pGAL1-BMH2*] (CDV235) cells carrying either the control plasmid pLC921 (strain 1) or plasmid pCDV994 (expressing $BMH2\text{-}HA^3$ from its own promoter; strain 2) were pregrown on SGal/Raf, transferred to SD medium, and grown exponentially (through repeated dilutions) for the times indicated. $Bmh2\text{-}HA^3$ and Bmh2 levels (in strains 1 and 2) were analyzed prior (time zero) and following (24 or 48 h) the transfer of the cells from SGal/Raf to SD medium via immunoblot analysis using anti-HA (top panel) and anti-Bmh2 (lower panel) antibodies (D). GFP-$Rim15^{C1176Y}$ was visualized 24 h following the transfer of the cells from SGal/Raf to SD medium (E). (**F**) Depletion of 14-3-3 proteins results in transcriptional activation of Rim15-dependent genes. *GRE1* and *HSP26* transcript levels were determined (via Northern blot analysis as described in Pedruzzi *et al*, 2000) at the times indicated following transfer of *bmh1*Δ *bmh2*Δ [*pGAL1-BMH2*] (SL1470) and *bmh1*Δ *bmh2*Δ *rim15*Δ [*pGAL1-BMH2*] (CDV235) cells from SGal/Raf to SD medium. Depletion of Bmh2 was monitored via immunoblot analysis using anti-Bmh2 antibodies (top panel).

tion, we found that Pho85 physically interacted with Rim15 in co-IP experiments (Figure 3A), and that Pho85, but not kinase-inactive $Pho85^{E53A}$ (Nishizawa *et al*, 1999), phosphorylated $Rim15^{KI}$ in the presence of the cyclin Pho80 (see Materials and methods for identification of Pho80; Figure 3B). In addition, Pho80–Pho85-mediated phosphorylation was significantly reduced (to 46.0% ± 6.6) by the introduction of the T1075A mutation in $Rim15^{KI}$ (Figure 3B), indicating that T1075 is a Pho80–Pho85 target *in vitro* (notably, the residual phosphorylation level in $Rim15^{KI\text{-}T1075A}$ suggests the presence of an additional site[s] in $Rim15^{KI}$ that may be targeted *in vitro* by Pho80–Pho85). To assess whether Pho80–Pho85 indeed phosphorylates T1075 in Rim15 within cells, we raised antibodies that were highly specific for a pT1075-containing peptide, as indicated by their ability to recognize GST-Rim15, but not GST-$Rim15^{T1075A}$, or phosphatase-treated GST-Rim15 (Figure 3C). Using these specific anti-pT1075 antibodies, we found that phosphorylation of T1075 in Rim15-myc[13] depends largely on the presence of Pho85 (Figure 3D). Thus, the T1075 residue in Rim15 is also a likely Pho80–Pho85 target *in vivo*. Taken together with our finding that loss of Pho85 or Pho80 (but not of Pcl1/Pcl2) resulted in the constitutive nuclear localization of GFP-$Rim15^{C1176Y}$ in 71% and 58% of the cells, respectively (Figure 3E), our data suggest a model in which the Pho80–Pho85 kinase promotes the cytoplasmic retention of Rim15 in exponentially growing cells principally through phosphorylation of the T1075 residue of the 14-3-3 site in Rim15.

The Pho80–Pho85 cyclin–CDK complex antagonizes the Rim15-dependent G_0 program

To address the physiological importance of our findings, we next examined the role of Pho85, if any, in the Rim15-dependent G_0 phenotypes (Reinders *et al*, 1998; Pedruzzi *et al*, 2003). We observed that loss of Pho80 or Pho85 significantly enhanced *GRE1-lacZ* induction (Figure 4A) and trehalose synthesis (Figure 4B) particularly following glucose limitation. Notably, the corresponding higher induction

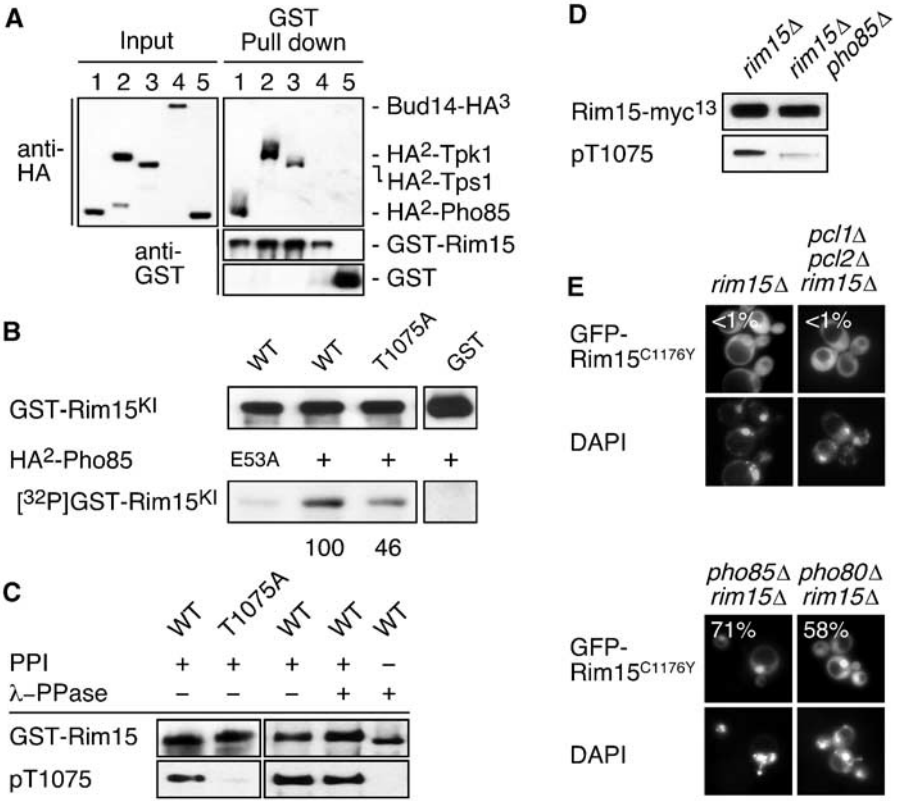

Figure 3 The Pho80–Pho85 cyclin–CDK phosphorylates the T1075-containing 14-3-3-binding site in Rim15 and stimulates its cytoplasmic retention. (**A**) Interaction between Rim15 and Pho85. GST-Rim15 (pNB566; lanes 1–4) and GST (YCpIF2-GST; lane 5) were precipitated from extracts prepared from wild-type (KT1961) cells coexpressing HA^2-Pho85 (pIP774; lanes 1 and 5), HA^2-Tpk1 (pCDV503; lane 2), HA^2-Tps1 (pAR502; lane 3), or Bud14-HA^3 (pFD662; lane 4). Cell lysates (Input) and GST pull-down fractions were subjected to PAGE and immunoblots were probed using anti-GST or anti-HA antibodies as indicated. Tpk1 and Tps1 (both previously identified as Rim15-interacting proteins; Reinders *et al*, 1998) served as positive controls, while Bud14 served as a negative control. (**B**) *In vitro* phosphorylation of T1075 in Rim15. GST-$Rim15^{KI}$ (pVW995), GST-$Rim15^{KI\text{-}T1075A}$ (pVW997), and GST (pGEX3X), expressed and purified from bacteria, were used as *in vitro* substrates (see top panel for input blot) in protein kinase assays using equal amounts of GST-Pho80 and either HA^2-Pho85 or protein kinase inactive HA^2-$Pho85^{E53A}$. The protein input bands (top panel) and the phosphorylation levels of the $Rim15^{KI}$ variants (lower panel) were quantified (see Materials and methods). The average ratio of [^{32}P]GST-$Rim15^{KI\text{-}T1075}$/GST-$Rim15^{KI\text{-}T1075}$ (from four independent experiments) is expressed in percent of the corresponding ratio for wild-type GST-$Rim15^{KI}$ (set at 100% following the deduction of the background signal in the E53A lane) and is indicated below the relevant lane. (**C**) *In vivo* phosphorylation of T1075 in Rim15. GST-Rim15 (WT; pNB566) and GST-$Rim15^{T1075A}$ (T1075A; pLC824) were purified from exponentially growing *rim15*Δ (IP31) cells and analyzed by immunoblotting (using either anti-GST antibodies or phospho-specific antibodies against Rim15-pT1075) following treatment with phosphatase inhibitors (PPI) alone or λ-phosphatase (λ-PPase) ± PPI. (**D**) Rim15-myc^{13} (pVW904) from exponentially growing *rim15*Δ (IP31) and *pho85*Δ *rim15*Δ (CDV201-3B) mutants were analyzed for phosphorylation of T1075 using Rim15-pT1075 phospho-specific antibodies. Equal amounts of the fusion proteins were verified by immunoblotting using anti-myc antibodies. (**E**) Localization of GFP-$Rim15^{C1176Y}$ (pFD633) in exponentially growing *rim15*Δ (IP31), *pcl1*Δ *pcl2*Δ *rim15*Δ (CDV237-9D), *pho85*Δ *rim15*Δ (CDV201-3B), and *pho80*Δ *rim15*Δ (CDV237-7A) mutant cells. The numbers indicate the percentage of cells with clear nuclear staining of the GFP-fusion protein; >200 cells were counted.

levels, which in the case of *pho85*Δ mutant cells also correlated with a slightly enhanced G_0 survival (Figure 4C), depended to a large extent on the presence of Rim15 (Figure 4A–C). Similarly, glycogen hyperaccumulation in *pho85*Δ mutants (Timblin *et al*, 1996) was largely dependent on the presence of Rim15 (Figure 4D). Together with our data presented above, these genetic results suggest a model in which the Pho80–Pho85 cyclin–CDK complex antagonizes the Rim15-dependent G_0 program by regulating the nuclear exclusion of Rim15.

We also found that the levels of both Pho80 and Pho85 drop significantly in the late post-diauxic shift phase (data not shown), suggesting that the Pho80–Pho85 kinase modulates the Rim15-dependent G_0 program in response to phosphate levels as long as residual carbon sources are available. This conclusion is confirmed by the findings that phosphate starvation resulted in the dephosphorylation of Rim15-pT1075 (Figure 4E), nuclear accumulation of GFP-$Rim15^{C1176Y}$ (Figure 4F), and, as recently published, Rim15 target gene expression (Swinnen *et al*, 2005). Thus, our physiologic, biochemical and genetic data are consistent with a model in which Rim15 represents a physiologically important Pho80–Pho85 cyclin–CDK target.

TORC1 also impinges on pT1075 in Rim15

We have previously shown that the nuclear accumulation of Rim15 is antagonized by the TORC1 pathway, and likely involves Rim15 hyper-phosphorylation (Pedruzzi *et al*, 2003). During our analyses of the various kinase-inactive Rim15 proteins, we observed that their electrophoretic mobility depended on the kinase activity of Rim15 itself and, therefore, likely reflects the autophosphorylation state of Rim15 (data not shown). A simple model could be that rapamycin-induced hyper-phosphorylation of Rim15 is a

consequence, rather than the cause, of Rim15 nuclear import and may be due to the activation of Rim15 in the presumably low PKA nuclear environment (Griffioen and Thevelein, 2002; Pedruzzi *et al*, 2003).

How then does TORC1 regulate the nucleocytoplasmic distribution of Rim15? In this respect, we observed that rapamycin treatment caused rapid dephosphorylation of pT1075 in Rim15 (Figure 4E), indicating that TORC1, like Pho80–Pho85, regulates the cytoplasmic retention of Rim15 primarily by controlling the phosphorylation state of its 14-3-3-binding site. The fact that rapamycin treatment does not significantly change the expression pattern of genes controlled by the Pho80–Pho85-regulated Pho4 transcription factor (e.g. *PHO5*, *PHO11*, and *PHO12*; Hardwick *et al*, 1999) argues against TORC1 acting upstream of Pho80–Pho85. Thus, TORC1, rather than impinging on Pho80–Pho85, may instead inhibit the activity of a pT1075-targeting phosphatase(s) and/or activate an alternative T1075-targeting kinase (Figure 5). In this context, our previous findings indicated that the known TORC1 effectors, including the type 2A-related protein phosphatase Sit4 and possibly also the type 2A protein phosphatases Pph21 and Pph22 (Di Como and Arndt, 1996; Jiang and Broach, 1999), may not be required for rapamycin-induced nuclear accumulation of Rim15 (Pedruzzi *et al*, 2003). Thus, unless these protein phosphatases redundantly control Rim15 function, our data suggest the existence of an additional, yet unidentified TORC1 effector(s) that regulates the phosphorylation state of T1075 in Rim15. Lastly, we would like to point out that TORC1 and Pho80–Pho85 localize to the cytoplasm and nucleus, respectively (Kaffman *et al*, 1998; Harris and Lawrence, 2003), and these kinases may therefore act on different pools of Rim15 (Figure 5). Our observation that rapamycin treatment and phosphate starvation act synergistically to cause a more complete depletion of GFP-Rim15^{C1176Y} from the cytoplasm supports this model (Figures 1A and 4F).

A final point remaining to be addressed is our previous finding that nuclear exclusion of Rim15 also requires the yeast PKB/Akt homolog Sch9. Analysis of the kinase insert sequence of Rim15 reveals three sites (S1004, S1044, and T1096), each of which is very similar to the consensus site phosphorylated by PKB/Akt (RXRXXS/T; Alessi *et al*, 1996) and conforms to a low-stringency 14-3-3-binding site (Yaffe *et al*, 2001). Given the dimeric nature of 14-3-3 proteins, it is possible that the kinase insert of Rim15 may engage in binding both monomeric subunits within a single 14-3-3 protein dimer, as previously shown to be the case for other proteins (Yaffe, 2002). Since our preliminary data indicate that Sch9 can phosphorylate Rim15^{KI} *in vitro*, it will be of interest to determine whether Sch9 phosphorylates an additional 14-3-3 site in Rim15^{KI}, which may act in concert with the 14-3-3-binding site flanking amino-acid residue T1075 to mediate tandem 14-3-3 binding.

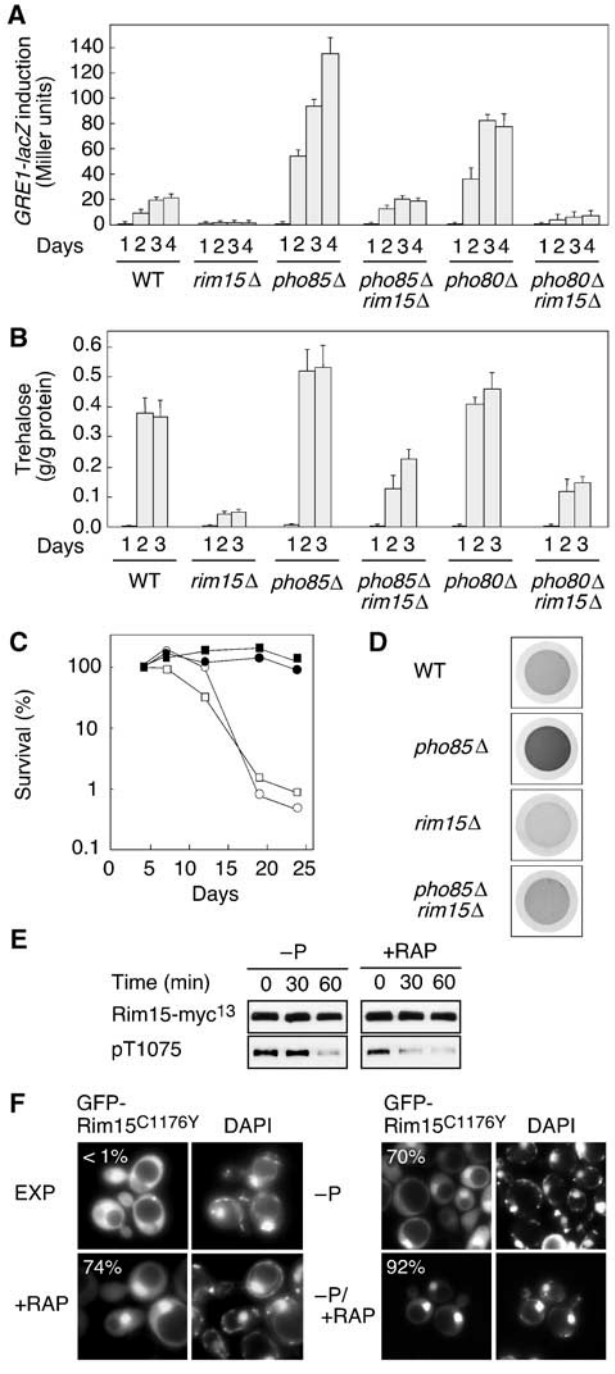

Figure 4 The Pho80–Pho85 cyclin–CDK complex antagonizes induction of Rim15-dependent G_0 traits. (**A**, **B**) Induction of *GRE1-lacZ* expression (from integrative plasmid pIP490; A) and trehalose levels (B; for method see Pedruzzi *et al*, 2000) as wild-type (KT1961), *rim15*Δ (IP31), *pho85*Δ (IP48-3C), *pho85*Δ *rim15*Δ (CDV201-3B), *pho80*Δ (CDV237-10C), and *pho80*Δ *rim15*Δ (CDV237-7A) mutant cells were grown to stationary phase on YPD medium. (**C**) Stationary phase survival of wild-type (●), *rim15*Δ (○), *pho85*Δ (■), and *pho85*Δ *rim15*Δ (□) mutant cells (for strains see [A, B]). (**D**) Glycogen levels in 4-day old batch cultures (visualized after exposure for 1 min to iodine vapor; for strains see [A, B]). (**E**) Both phosphate starvation and rapamycin treatment reduce the extent of phosphorylation of the T1075 residue in Rim15. Exponentially growing *rim15*Δ (IP31) cells expressing Rim15-myc[13] (pVW904) were starved for phosphate (−P) or treated with rapamycin (+RAP) for the indicated times. Detection of fusion protein levels and pT1075 were as in Figure 3D. (**F**) Exponentially growing *rim15*Δ (IP31) cells expressing GFP-Rim15^{C1176Y} (pFD633; EXP) were treated for 45 min with rapamycin (+RAP), or submitted for 45 min to phosphate starvation in the absence (−P) or in the presence (−P/+RAP) of rapamycin and subsequently visualized by fluorescence microscopy. The numbers indicate the percentage of cells with clear nuclear staining of the GFP-fusion protein; >200 cells were counted.

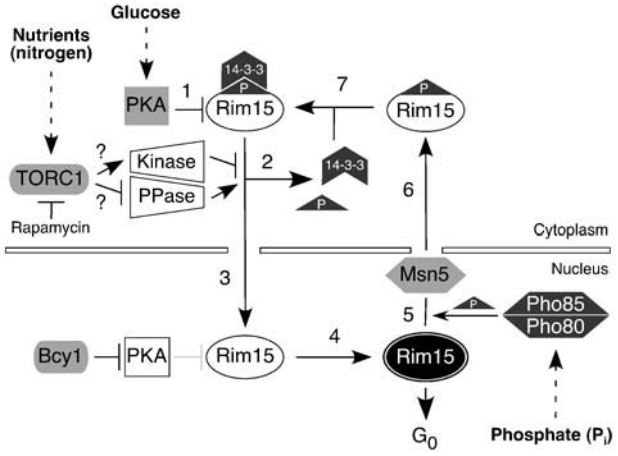

Figure 5 Model for the regulation of Rim15 by nutrient-sensory kinases. Cytoplasmic Rim15, anchored through its binding to 14-3-3 proteins, is kept inactivate through PKA-mediated phosphorylation (1). TORC1 inactivation results (either due to the activation of a phosphatase[s] and/or inactivation of a protein kinase) in dephosphorylation of pT1075 in Rim15 with concomitant abrogation of cytoplasmic retention of Rim15 by 14-3-3 proteins (2). Following its nuclear import (3), Rim15 presumably escapes from further PKA-mediated inhibition (4). Active Rim15 (drawn in black) induces the G_0 program, initiates an autophosphorylation process (illustrated with a circle around Rim15), and accelerates its Msn5-mediated nuclear export. The Pho80–Pho85 cyclin–CDK complex phosphorylates T1075 of Rim15 (5), thereby promoting (following export of Rim15; 6) the re-association between Rim15 and 14-3-3 proteins in the cytoplasm (7). The nutrient sensing protein kinases PKA, TOR (in TORC1), and Pho80-Pho85 sense glucose, nutrients (nitrogen), and phosphate (P_i), respectively (Wilson and Roach, 2002). See text for further details.

In conclusion, we have identified a new regulatory mechanism by which the availability of phosphate modulates the G_0 program in yeast. We propose that the PAS kinase Rim15, in addition to integrating carbon and/or nitrogen source signals via the PKA, TORC1, and Sch9 nutrient-sensory kinases (Pedruzzi *et al*, 2003), also integrates information on the availability of phosphate via the Pho80-Pho85 cyclin–CDK complex to properly orchestrate the G_0 program, a key developmental process in eukaryotic cells.

Materials and methods

Yeast strains, media and genetic techniques

The *rim15*Δ strains IP31 and CDV115 and their corresponding wild-type strains KT1960/1 and W303-1A, respectively, have been described earlier (Thomas and Rothstein, 1989; Pedruzzi *et al*, 2003). The *msn5*Δ strain YBL029, which is isogenic to PAY20 and W303-1A (Blondel *et al*, 1999), was a kind gift of Dr M Peter. Polymerase chain reaction (PCR)-based gene deletions (*pcl1*Δ::*kanMX2*, *pcl2*Δ::*kanMX2*, *pho80*Δ::*kanMX2*, *pho85*Δ::*kanMX2*, and *rim15*Δ::*kanMX2* transformed into KT1960 and/or KT1961) were carried out as described (Longtine *et al*, 1998). The corresponding single mutants (all in same isogenic background) were used to construct IP48-3C (*pho85*Δ), CDV201-3B (*pho85*Δ *rim15*Δ), CDV237-10C (*pho80*Δ), CDV237-7A (*pho80*Δ *rim15*Δ), and CDV237-9D (*pcl1*Δ *pcl2*Δ *rim15*Δ) by a series of repeated combinatorial mating and sporulation of the resulting diploids. Gene deletions were confirmed by PCR with gene-specific primers. PCR-based deletion of *RIM15* (using a *rim15*Δ::*kanMX2* cassette) in strain SL1470 (*bmh1*Δ *bmh2*Δ [p*GAL1-BMH2*]; described in Gelperin *et al*, 1995) yielded strain CDV235. The isogenic strains BY236 (wild type), BY714 (*pcl1*Δ *pcl2*Δ *pcl5*Δ *pcl9*Δ *clg1*Δ), BY708 (*pcl1*Δ *pcl2*Δ *pcl5*Δ *pcl9*Δ), BY637 (*pcl1*Δ *pcl2*Δ *pcl5*Δ *clg1*Δ), BY634 (*pcl1*Δ *plc2*Δ), and BY490 (*pho80*Δ) have been previously described (Measday *et al*, 1997). Strains were grown at 30°C in standard rich medium with 2% glucose (YPD) or synthetic medium with 2% glucose (SD), 4% galactose (SGal), or 2% raffinose (SRaf) as carbon source (Burke *et al*, 2000). High- and no-phosphate media were described earlier (Kaffman *et al*, 1998). Rapamycin was added to the media at a final concentration of 2 μg ml^{-1}. Standard yeast genetic manipulations were used (Burke *et al*, 2000). DNA was stained with 4,6-diamidino-2-phenylindole (DAPI), which was added to the cultures (4 h prior to fluorescence microscopy) at a concentration of 1 μg ml^{-1}.

Plasmids

Full-length Rim15, Rim15^{K823Y}, Rim15^{C1176Y}, Rim15$^{C1176Y/T1075A}$, and Rim15$^{C1176Y/\Delta KI}$ (in which the kinase insert domain encompassing amino acids 952–1138 is deleted; ΔKI) were expressed as GFP-tagged versions under the control of the constitutive *ADH1* promoter from low copy number plasmids pFD846, pFD1008, pFD633, pVW1017, and pVW1068, respectively. In addition, full-length Rim15 and Rim15^{T1075A} were expressed as GST-tagged versions under the control of the *GAL1* promoter from the high copy number plasmids pNB566 and pLC824, respectively. Finally, full-length Rim15 was also expressed as myc^{13}-tagged version under the control of the *TDH3* promoter from high copy number plasmids pVW904. Plasmids expressing epitope-tagged variants of full-length Rim15 were constructed with the QuickChange Site-Directed Mutagenesis Kit (Stratagene) using appropriate primers that introduced the K823Y-, C1176Y-, and/or T1075A-encoding mutations in the corresponding parent plasmids (pFD846 and pNB566). To express a GST-tagged version of the kinase insert of Rim15 (Rim15^{KI}) under the control of the *tetO7* promoter, an *Not*I–*Sal*I fragment, containing the 672 nucleotides downstream of and including the *GST* start codon (Reinders *et al*, 1998), and a PCR-generated *Sal*I–*Pst*I fragment, encoding amino-acid residues 944 to 1149 of Rim15, were coligated with *Not*I–*Pst*I-cut pCM184 (Garí *et al*, 1997), thus creating pVW900 (*tetO7-GST-RIM15^{KI}*). Plasmid pVW902 (*tetO7-GST-RIM15$^{KI\text{-}T1075A}$*) was obtained by site-directed mutagenesis (see above) of *RIM15^{KI}* in pVW900 using appropriate primers that introduced the T1075A-encoding mutation. For expression of GST-Rim15^{KI} in *Escherichia coli* (BL21; Stratagene), a PCR-generated *Bam*HI–*Eco*RI fragment, encoding amino-acid residues 944 to 1149 of Rim15, was ligated into *Bam*HI–*Eco*RI-digested pGEX3X (Amersham) to yield pVW995 (*P$_{tac}$-GST-RIM15^{KI}*). Plasmid pVW997 (*P$_{tac}$-GST-RIM15$^{KI\text{-}T1075A}$*) was obtained by site-directed mutagenesis (see above) of *RIM15^{KI}* in pVW995 using appropriate primers that introduced the T1075A-encoding mutation. Bmh2-HA^3 was expressed under the control of its own promoter from either a high-copy number plasmid (pTB419), which was kindly provided by Dr M Hall (Beck and Hall, 1999), or a low copy number plasmid (pCDV994) that was created by cloning the *Bam*HI–*Hind*III-digested, *BMH2-HA^3* carrying fragment of pTB419 at the *Bam*HI–*Hind*III sites of pLC921, a YCplac33 (Gietz and Sugino, 1988) version that carries the *natMX4* cassette-containing *Eco*RI–*Hind*III fragment of pAG25 (Goldstein and McCusker, 1999) in its polylinker region. Full-length Tpk1, Tps1 and Pho85 were expressed as HA^2-tagged versions under the control of the *GAL1* promoter from plasmids pCDV503 (*GAL1-HA^2-TPK1*), pAR502 (*GAL1-HA^2-TPS1*) and pIP774 (*GAL1-HA^2-PHO85*), respectively. Full-length Bud14 was expressed as HA^3-tagged version under its own promoter from plasmid pFD662 (*BUD14-HA^3*). In addition, full-length Pho85 was also expressed as a HA^2-tagged version under the control of the *tetO7* promoter from plasmid pVW883 (*tetO7-HA^2-PHO85*). Plasmid pVW884 (*tetO7-HA^2-PHO85^{E53A}*) was obtained by site-directed mutagenesis (see above) of *PHO85* in pVW883 using appropriate primers to introduce the kinase-inactivating E53A-encoding mutation. The integrative pLS9-*GRE1-lacZ* plasmid (pIP490) was constructed by cloning a PCR-generated *Eco*RI fragment, containing the 778 nucleotides upstream of the *GRE1* start codon, into the *Eco*RI site of pLS9 (Sarokin and Carlson, 1986). Plasmids YCpIF2-GST and p2466, which allow expression of GST-Pho80 under the control of the *CUP1* promoter, have been described earlier (Reinders *et al*, 1998; Tan *et al*, 2003).

Kinase-inactivating K823Y and C1176Y mutations in Rim15

The K823Y substitution replaces the invariant lysine in kinase subdomain II of Rim15 with tyrosine and results in an ATP-binding deficient version of Rim15 (Vidan and Mitchell, 1997; Reinders *et al*, 1998). During detailed analyses of our original GFP-Rim15

clone (pFD633; Pedruzzi *et al*, 2003), we discovered that it acquired a fortuitous point mutation (G3527A) that changes the cysteine residue at position 1176 to a tyrosine (C1176Y), located immediately downstream of the almost invariant glycine of the kinase catalytic sub-domain IX (Hanks *et al*, 1988). Subsequent experiments indeed revealed that the C1176Y mutation results in inactivation of the Rim15 protein kinase activity (data not shown). Consistent with our previous results, GFP-Rim15^{C1176Y} accumulates in the nuclei of glucose-limited and rapamycin-treated *rim15*Δ cells (Figure 1A; Pedruzzi *et al*, 2003). However, the presence of a functional (genomic or plasmid-expressed) Rim15 kinase efficiently prevents the observed nuclear accumulation of Rim15 (data not shown). While these new findings do not affect our previous conclusions (Pedruzzi *et al*, 2003), they provide a basis for the present study of cytoplasmic retention and/or nuclear import of GFP-Rim15.

Identification of the Pho80 cyclin

We expected that loss of the Pho85 partner cyclins, either alone or in combination, should phenocopy the loss of Pho85 with respect to hyper-induction of Rim15-dependent genes. Indeed, we found that loss of the cyclin Pho80 (in strain BY490), but none of various combinations of other cyclin mutations (including *pcl1*Δ *pcl2*Δ *pcl5*Δ *pcl9*Δ *clg1*Δ [BY714], *pcl1*Δ *pcl2*Δ *pcl5*Δ *pcl9*Δ [BY708], *pcl1*Δ *pcl2*Δ *pcl5*Δ *clg1*Δ [BY637], and *pcl1*Δ *plc2*Δ [BY634]), resulted in hyperactivation of *HSP26*, *SSA3*, and *GRE1* transcription when assayed during the early diauxic shift phase (data not shown).

GST pull-down, immunoprecipitation, immunoblot analyses, and phospho-specific antibodies

To perform coprecipitation experiments between Rim15 and Pho85, strain KT1960 was cotransformed with pNB566 or YCpIF2-GST (expressing GST-Rim15 or GST under the *GAL1* promoter, respectively) and either pIP774, pCDV503, pAR502, or pFD662, which express HA^2-Pho85, HA^2-Tpk1, HA^2-Tps1, or Bud14-HA^3, respectively. Induction of *GAL1*-driven expression and cell lysis were essentially performed as described (Lenssen *et al*, 2005). GST and GST-tagged Rim15 were purified from clarified extracts using glutathione sepharose 4B beads (Amersham Biosciences). Bound proteins were eluted with sample buffer (5 min, 95°C) and subjected to standard immunoblot analysis for detection of coprecipitated HA^2-Pho85, HA^2-Tpk1 and HA^2-Tps1. For co-IP experiments between Bmh2 and Rim15^{KI} or Rim15$^{KI\text{-}T1075}$, strain W303-1A was cotransformed with pTB419 expressing Bmh2-HA^3 under the control of its own promoter and pVW900 or pVW902, which express GST-Rim15^{KI} or GST-Rim15$^{KI\text{-}T1075A}$, respectively, under the control of the *tetO7* promoter. To allow expression of the *tetO7*-controlled genes, cells were grown for at least six generations in exponential growth phase (OD_{600}<1.0) in the absence of doxycycline. Subsequently, cells were lysed (see above) and HA-tagged Bmh2 proteins were purified from clarified extracts with the protein G-agarose IP kit (Roche Diagnostics GmbH) following the manufacturer's instructions using monoclonal mouse anti-HA antibodies (HA.11; Covance). Bound proteins were eluted (as above) and subjected to standard immunoblot analysis for detection of co-precipitated GST-Rim15^{KI} and GST-Rim15$^{KI\text{-}T1075A}$. Dephosphorylation of GST-Rim15 (purified from whole-cell extracts; see above) was carried out by a 30-min incubation at 30°C with 1 U of λ-phosphatase (Biolabs, NewEngland). In control reactions, phosphatase inhibitors (10 mM NaF, 10 mM Na-orthovanadate, 10 mM *p*-NO_2-phenylphosphate, 10 mM β-glycerophosphate, and 10 mM Na-pyrophosphate) were added. Antibodies against Rim15 phosphorylated on T1075 were raised against a phosphorylated synthetic peptide (S-R-S-S-pT-P-P-L-A-N-P-T; where pT represents phosphothreonine 1075 of Rim15), adsorbed with the unphosphorylated form of the peptide, and affinity-purified with the phosphorylated peptide by Eurogentec.

Protein kinase assays and quantification of substrate phosphorylation

To assay *in vitro* phosphorylation of Rim15 by Pho85, HA^2-Pho85 (pVW883) and HA^2-Pho85^{E53A} (pVW884), fusion proteins were expressed in (following growth for at least six generations in exponential growth phase in the absence of doxycycline) and purified from *rim15*Δ *pho85*Δ (CDV201-3B) cells. Following this, cells were disrupted by vortexing in lysis buffer (50 mM Tris–HCl, pH 7.5, 0.15 M NaCl, 0.5 mM EDTA, 0.1% NP-40, 10% glycerol, 1 mM PMSF, 1 mM DTT, one tablet of Complete Protease Inhibitor Cocktail [CPIC; Roche Diagnostics GmbH] per 50 ml, and phosphatase inhibitors [see above] in the presence of acid-washed glass beads. HA-tagged Pho85 and Pho85^{E53A} proteins were purified as outlined above for the HA-tagged Bmh2 protein. Kinase assays were performed with HA^2-Pho85- and HA^2-Pho85^{E53A}-bound beads at 30°C for 30 min in kinase buffer (50 mM Tris–HCl, pH 7.5, 20 mM $MgCl_2$, 1 mM DTT, 1 mM ATP, one tablet of CPIC per 50 ml, and 10 μCi γ-ATP) containing 50 ng of GST-Pho80 (purified from *rim15*Δ *pho85*Δ (CDV201-3B) cells; see also Tan *et al*, 2003) and the indicated Rim15-derived substrates (purified from *E. coli*). Reactions were stopped by adding SDS-gel loading buffer and boiling for 5 min and then subjected to SDS–PAGE. Gels were dried and exposed to X-ray film. Substrate phosphorylation levels were quantified using a PhosphorImager (Cyclone Phosphor System; PerkinElmer) and analysed with OptiQuant Image Analysis software (Packard). Digital images of immunoblots were acquired with a CanoScan LiDE scanner (Canon) and Photoshop 7.0 (Adobe) and densitometric analysis of protein bands was done with OptiQuant Image Analysis software.

Acknowledgements

We thank Drs B Andrews, J Cannon, M Hall, and S Lemmon for providing yeast strains, plasmids, and/or anti-Bmh2 antibodies, R Bisig for technical assistance, and Drs C Georgopoulos and R Loewith for critical reading of the manuscript. CDV is supported by the Swiss National Science Foundation grant 631-062731.00 and the Canton of Geneva.

References

Alessi DR, Caudwell FB, Andjelkovic M, Hemmings BA, Cohen P (1996) Molecular basis for the substrate specificity of protein kinase B; comparison with MAPKAP kinase-1 and p70 S6 kinase. *FEBS Lett* **399:** 333–338

Beck T, Hall MN (1999) The TOR signalling pathway controls nuclear localization of nutrient-regulated transcription factors. *Nature* **402:** 689–692

Blondel M, Alepuz PM, Huang LS, Shaham S, Ammerer G, Peter M (1999) Nuclear export of Far1p in response to pheromones requires the export receptor Msn5p/Ste21p. *Genes Dev* **13:** 2284–2300

Burke D, Dawson D, Stearns T (2000) *Methods in Yeast Genetics*. New York: Cold Spring Harbor Laboratory Press

Cameroni E, Hulo N, Roosen J, Winderickx J, De Virgilio C (2004) The novel yeast PAS kinase Rim15 orchestrates G_0-associated antioxidant defense mechanisms. *Cell Cycle* **3:** 462–468

Carroll AS, Bishop AC, DeRisi JL, Shokat KM, O'Shea EK (2001) Chemical inhibition of the Pho85 cyclin-dependent kinase reveals a role in the environmental stress response. *Proc Natl Acad Sci USA* **98:** 12578–12583

Carroll AS, O'Shea EK (2002) Pho85 and signaling environmental conditions. *Trends Biochem Sci* **27:** 87–93

DeRisi JL, Iyer VR, Brown PO (1997) Exploring the metabolic and genetic control of gene expression on a genomic scale. *Science* **278:** 680–686

Di Como CJ, Arndt KT (1996) Nutrients, via the Tor proteins, stimulate the association of Tap42 with type 2A phosphatases. *Genes Dev* **10:** 1904–1916

Garí E, Piedrafita L, Aldea M, Herrero E (1997) A set of vectors with a tetracycline-regulatable promoter system for modulated gene expression in *Saccharomyces cerevisiae*. *Yeast* **13:** 837–848

Gelperin D, Weigle J, Nelson K, Roseboom P, Irie K, Matsumoto K, Lemmon S (1995) 14-3-3 proteins: potential roles in vesicular transport and Ras signaling in *Saccharomyces cerevisiae*. *Proc Natl Acad Sci USA* **92:** 11539–11543

Gietz RD, Sugino A (1988) New yeast-*Escherichia coli* shuttle vectors constructed with *in vitro* mutagenized yeast genes lacking six-base pair restriction sites. *Gene* **74:** 527–534

Goldstein AL, McCusker JH (1999) Three new dominant drug resistance cassettes for gene disruption in *Saccharomyces cerevisiae*. *Yeast* **15:** 1541–1553

Gray JV, Petsko GA, Johnston GC, Ringe D, Singer RA, Werner-Washburne M (2004) 'Sleeping beauty': quiescence in *Saccharomyces cerevisiae*. *Microbiol Mol Biol Rev* **68:** 187–206

Griffioen G, Thevelein JM (2002) Molecular mechanisms controlling the localisation of protein kinase A. *Curr Genet* **41:** 199–207

Hanks SK, Quinn AM, Hunter T (1988) The protein kinase family: conserved features and deduced phylogeny of the catalytic domains. *Science* **241:** 42–52

Hardwick JS, Kuruvilla FG, Tong JK, Shamji AF, Schreiber SL (1999) Rapamycin-modulated transcription defines the subset of nutrient-sensitive signaling pathways directly controlled by the Tor proteins. *Proc Natl Acad Sci USA* **96:** 14866–14870

Harris TE, Lawrence Jr JC (2003) TOR signaling. *Sci STKE* **212:** re15

Ichimura T, Kubota H, Goma T, Mizushima N, Ohsumi Y, Iwago M, Kakiuchi K, Shekhar HU, Shinkawa T, Taoka M, Ito T, Isobe T (2004) Transcriptomic and proteomic analysis of a 14-3-3 gene-deficient yeast. *Biochemistry* **43:** 6149–6158

Jiang Y, Broach JR (1999) Tor proteins and protein phosphatase 2A reciprocally regulate Tap42 in controlling cell growth in yeast. *EMBO J* **18:** 2782–2792

Kaffman A, Rank NM, O'Neill EM, Huang LS, O'Shea EK (1998) The receptor Msn5 exports the phosphorylated transcription factor Pho4 out of the nucleus. *Nature* **396:** 482–486

Lenssen E, James N, Pedruzzi I, Dubouloz F, Cameroni E, Bisig R, Maillet L, Werner M, Roosen J, Petrovic K, Winderickx J, Collart MA, De Virgilio C (2005) The Ccr4-Not complex independently controls both Msn2-dependent transcriptional activation—via a newly identified Glc7/Bud14 type I protein phosphatase module—and TFIID promoter distribution. *Mol Cell Biol* **25:** 488–498

Lillie SH, Pringle JR (1980) Reserve carbohydrate metabolism in *Saccharomyces cerevisiae*: responses to nutrient limitation. *J Bacteriol* **143:** 1384–1394

Longtine MS, McKenzie III A, DeMarini DJ, Shah NG, Wach A, Brachat A, Philippsen P, Pringle JR (1998) Additional modules for versatile and economical PCR-based gene deletion and modification in *Saccharomyces cerevisiae*. *Yeast* **14:** 953–961

Martin DE, Hall MN (2005) The expanding TOR signaling network. *Curr Opin Cell Biol* **17:** 158–166

Measday V, Moore L, Retnakaran R, Lee J, Donoviel M, Neiman AM, Andrews B (1997) A family of cyclin-like proteins that interact with the Pho85 cyclin-dependent kinase. *Mol Cell Biol* **17:** 1212–1223

Moriya H, Shimizu-Yoshida Y, Omori A, Iwashita S, Katoh M, Sakai A (2001) Yak1p, a DYRK family kinase, translocates to the nucleus and phosphorylates yeast Pop2p in response to a glucose signal. *Genes Dev* **15:** 1217–1228

Nishizawa M, Katou Y, Shirahige K, Toh-e A (2004) Yeast Pho85 kinase is required for proper gene expression during the diauxic shift. *Yeast* **21:** 903–918

Nishizawa M, Suzuki K, Fujino M, Oguchi T, Toh-e A (1999) The Pho85 kinase, a member of the yeast cyclin-dependent kinase (Cdk) family, has a regulation mechanism different from Cdks functioning throughout the cell cycle. *Genes Cells* **4:** 627–642

O'Neill EM, Kaffman A, Jolly ER, O'Shea EK (1996) Regulation of PHO4 nuclear localization by the PHO80–PHO85 cyclin–CDK complex. *Science* **271:** 209–212

Ogawa N, DeRisi J, Brown PO (2000) New components of a system for phosphate accumulation and polyphosphate metabolism in *Saccharomyces cerevisiae* revealed by genomic expression analysis. *Mol Biol Cell* **11:** 4309–4321

Pedruzzi I, Bürckert N, Egger P, De Virgilio C (2000) *Saccharomyces cerevisiae* Ras/cAMP pathway controls post-diauxic shift element-dependent transcription through the zinc finger protein Gis1. *EMBO J* **19:** 2569–2579

Pedruzzi I, Dubouloz F, Cameroni E, Wanke V, Roosen J, Winderickx J, De Virgilio C (2003) TOR and PKA signaling pathways converge on the protein kinase Rim15 to control entry into G_0. *Mol Cell* **12:** 1607–1613

Reinders A, Bürckert N, Boller T, Wiemken A, De Virgilio C (1998) *Saccharomyces cerevisiae* cAMP-dependent protein kinase controls entry into stationary phase through the Rim15p protein kinase. *Genes Dev* **12:** 2943–2955

Sarokin L, Carlson M (1986) Short repeated elements in the upstream regulatory region of the *SUC2* gene of *Saccharomyces cerevisiae*. *Mol Cell Biol* **6:** 2324–2333

Schmelzle T, Beck T, Martin DE, Hall MN (2004) Activation of the RAS/cyclic AMP pathway suppresses a TOR deficiency in yeast. *Mol Cell Biol* **24:** 338–351

Schneper L, Düvel K, Broach JR (2004) Sense and sensibility: nutritional response and signal integration in yeast. *Curr Opin Microbiol* **7:** 624–630

Swinnen E, Rosseels J, Winderickx J (2005) The minimum domain of Pho81 is not sufficient to control the Pho85-Rim15 effector branch involved in phosphate starvation-induced stress responses. *Curr Genet* **48:** 18–33

Tamaskovic R, Bichsel SJ, Hemmings BA (2003) NDR family of AGC kinases—essential regulators of the cell cycle and morphogenesis. *FEBS Lett* **546:** 73–80

Tan YS, Morcos PA, Cannon JF (2003) Pho85 phosphorylates the Glc7 protein phosphatase regulator Glc8 *in vivo*. *J Biol Chem* **278:** 147–153

Thevelein JM, de Winde JH (1999) Novel sensing mechanisms and targets for the cAMP-protein kinase A pathway in the yeast *Saccharomyces cerevisiae*. *Mol Microbiol* **33:** 904–918

Thomas BJ, Rothstein R (1989) Elevated recombination rates in transcriptionally active DNA. *Cell* **56:** 619–630

Timblin BK, Bergman LW (1997) Elevated expression of stress response genes resulting from deletion of the PHO85 gene. *Mol Microbiol* **26:** 981–990

Timblin BK, Tatchell K, Bergman LW (1996) Deletion of the gene encoding the cyclin-dependent protein kinase Pho85 alters glycogen metabolism in *Saccharomyces cerevisiae*. *Genetics* **143:** 57–66

Vidan S, Mitchell AP (1997) Stimulation of yeast meiotic gene expression by the glucose-repressible protein kinase Rim15p. *Mol Cell Biol* **17:** 2688–2697

Wilson WA, Roach PJ (2002) Nutrient-regulated protein kinases in budding yeast. *Cell* **111:** 155–158

Yaffe MB (2002) How do 14-3-3 proteins work? Gatekeeper phosphorylation and the molecular anvil hypothesis. *FEBS Lett* **513:** 53–57

Yaffe MB, Leparc GG, Lai J, Obata T, Volinia S, Cantley LC (2001) A motif-based profile scanning approach for genome-wide prediction of signaling pathways. *Nat Biotechnol* **19:** 348–353

